(14) de Gennes, P. G. *Scaling Concepts in Polymer Physics*; Cornell University Press: Ithaca, NY, 1978.
(15) Silberberg, A. *Pure Appl. Chem.* **1971**, *26*, 583.
(16) *Handbook of Chemistry and Physics*; Weast, R. C., Ed.; CRC Press: Boca Raton, FL; p E-360.
(17) It should be emphasized that the ellipsometry is useful in conjunction with the known polymer concentration profile function. That is our data are compared with only those concentration profiles used previously.
(18) Schaefer, D. W.; Joanny, J. F.; Pincus, P. *Macromolecules* **1980**, *13*, 1280.
(19) Kim, M. W.; Peiffer, D. G. *J. Chem. Phys.* **1985**, *83*(8), 4159.

Homopolygalacturonan Nitroxyl Amides: Matrix Deformation Induced Motional Perturbations of Cell Wall Polyuronides

W. Chamulitrat and P. Irwin*

Eastern Regional Research Center, Agricultural Research Service, U.S. Department of Agriculture, 600 East Mermaid Lane, Philadelphia, Pennsylvania 19118.
Received August 29, 1988; Revised Manuscript Received September 9, 1988

ABSTRACT: Galacturonic acid containing polymers in intact higher plant cortical cell walls were nitroxyl labeled at the C_6 position via an amide linkage in order to investigate the microscopic structure of the complex cell wall network in the dry and hydrated solid states. Cross-polarization and magic angle sample spinning NMR and EPR data indicate that the paramagnetic labels covalently attach near hydrophobic methyl ester domains, which, in turn, induce steric hindrance of the nitroxyl amide's motions. The energy of activation for internal motions of demethylated labeled cell wall powders was less than that of the native labeled matrix. Activation energies increased proportionally for these motions as a function of increasing the level of bound Ca^{2+}. EPR spectra of equilibrium-hydrated cell walls indicated that there were relatively large proportions of the galacturonosidic matrix in highly aggregated, possibly helical, domains due to steric and/or cross-linking effects occurring in the cell wall lattice. The fraction of weakly immobilized (isotropic) components, from composite EPR spectral envelopes at various levels of hydration, was obtained with pectin methyl esterase and alkali (solubilizes certain β-D-glucans and saponifies methyl esters) treated cell walls. The relative concentration of weakly immobilized EPR components was utilized as a measure of the interaction of the free sugar acid blocks with their surrounding polymer network. Enzymatically demethylated cell walls had an intermolecular coupling constant, derived from Fujita–Doolittle plots, 58% smaller than the native material, which provides strong evidence that methyl ester groups modulate segmental motion in the cell wall matrix via hydrophobic interactions. Divalent cationic cross-linkages between adjacent homopolygalacturonan blocks displayed a positively cooperative effect on an intermolecular coupling parameter as the fraction of binding sites being filled with Ca^{2+} increased. The latter observation argues that the binding of Ca^{2+} results in greater matrix deformation than can be explained by a random spatial distribution of the bound cations.

Introduction

The primary cell wall of most higher plants is believed to be a biphasic structure consisting of a skeleton of cellulose microfibrils held together by a rigid gellike lattice (the matrix polysaccharides).[1,2] The matrix components, which contribute about two-thirds to the total primary cell wall and middle lamellar mass, are polyhydroxy, hydrophilic, mostly carbohydrate macromolecules, which are extensively hydrated in vivo. Poly(galacturonic acid)-containing polymer species are one of the most important structural matrix polysaccharides in the stabilization of the wall lattice.[3,4] Little is understood about these sugar acid polymers' higher order structure[5] or how they form ordered arrays with a minimization of interaction energy in the native state.[6]

The associations of various polysaccharides in gels have been investigated,[7] and different types of interaction profiles between macromolecules can be distinguished. A gel structure has been proposed to exist through the exclusion of incompatible coils and the realignment of stiff structures with more compatible geometries to form mixed aggregates. However, the gel structure of polymer chains in cell wall matrices appears to be much more complicated because of the large manifold of weak forces interacting between the various matrix polysaccharides. In our laboratory, we have investigated[8] hydration-induced flexibility in a model system (e.g., poly(galacturonic acid), PGA) for the matrix components of higher plant cell walls. Thus, it is now possible to investigate more extensively the relative polymer flexibility of the sugar acid matrix components in the cell wall lattice as a function of various weak intermolecular forces. Such knowledge will assist in the elucidation of the higher order structure of certain cell wall polysaccharides in their native state as well as their physicochemical characteristics in the wall lattice.

The primary structure of cortical cell wall polymers of *Malus pumila* has been characterized in some detail.[9-12] The galacturonic acid containing matrix polymers exist in a form referred to as pectin or pectinic acid and are based on a backbone rich in α-(1→4)-linked D-galacturonic acid (the homopolygalacturonans) interspersed with (1→2)- and (1→2,4)-substituted L-rhamnose moieties, which are usually further linked with other neutral sugar polymers, forming "hairy" domains or side chains. The carboxyl groups of some of the galacturonan residues are methyl esterified to various degrees. Divalent cations have been shown to induce gelation in sugar acid macromolecules whereupon the ion–polyuronide lattice has been proposed to be represented as the "egg box" model as shown by circular dichroism[13,14] for solutions and by electron paramagnetic resonance[15] in intact higher plant cell wall matrices. Cell wall sugar acid domains have been found to contain up to 25–30% neutral sugars and 70–75% galacturonic acid monomer equivalents.[16] The high proportion of uronic acid residues is advantageous since our technique

* To whom correspondence should be addressed.

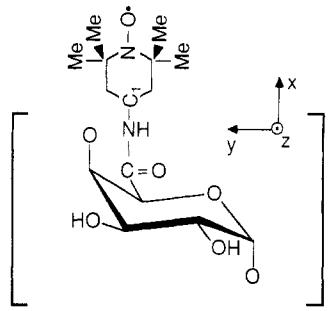

Figure 1. Schematic of a nitroxyl amide spin-labeled galacturonan with the magnetic axes of the electron spin provided.

involves the specific reaction of the uronic acid carboxyl groups with a spin label to form nitroxyl amides (Figure 1).[8,17] In this work, we report perturbations in the higher order structure and mobility of the sugar acid containing matrix polysaccharide chains induced by ionic cross-bonding as well as other weak forces.

Experimental Section

Malus pumila fruits (cv Golden Delicious) were obtained from the Beltsville Agricultural Research Center. Fruits were picked, randomized, and subsequently processed as described previously.[18] The cortical cell wall powders, which were stored in absolute EtOH at 2 °C, were critical point dried prior to further experimental processing.

Cell Wall Structural Modification. A specific methyl esterase (pectin methyl esterase, PME; Lot P6763) was purchased from Sigma Chemical Co., St. Louis, MO. Additional purification of this enzyme was not performed since the major contaminant, polygalacturonase, should not be active under the conditions (pH 7–8) that the esterase experiments were performed.[19] To test for any significant hydrolase activity at pH 7, we ran several PME experiments with 1% [w/v] citrus pectin (ca. 70% methyl esterified) under identical conditions to the PME cell wall experiments; no increase in reducing end groups was noted as a function of time, therefore indicating that no uronosyl hydrolases were active under these conditions. PME-treated cell walls were prepared by adding 300 units of PME (1 unit = 10^{-6} mol of methyl ester functional groups cleaved/min) to 720 mg of cell walls suspended in 40 mL of 0.1 N NaCl, and the mixture was slowly stirred for approximately 20 h; control samples were prepared identically but with a heat denatured enzyme. The PME-treated cell wall matrices were then spin labeled with 4-amino-2,2,6,6-tetramethylpiperidinyl-1-oxyl (4AT) as reported previously.[8,17] A third treatment consisted of the extraction of hemicellulose, the other major matrix polysaccharide, from the primary cell wall using standard techniques.[20] The cell wall materials prepared in this way were subsequently washed with 0.01 N HCl in 60% EtOH:H_2O, dehydrated in absolute EtOH, critical point dried, and labeled with nitroxyl spins.[17]

Cell Wall Spin-Labeling Conditions. For each cell wall sugar acid spin-labeling reaction,[17] 250 mg of dry cell walls was suspended in 50 mL of 60% EtOH:H_2O and gently agitated. This solvent system was used in order to avoid the solubilization of the cell wall matrix as could occur in pure H_2O. To this suspension was added 58 mg of 4AT and the pH slowly adjusted to 4.75 with acidified 60% EtOH:H_2O (ca. 0.1 N). Aliquots of approximately 30 mg of 1-ethyl-3-(3-(dimethylamino)propyl)carbodiimide (EDC) were added to the reaction mixture slowly at $^1/_2$-1-h intervals to a total of 250 mg. Upon stabilization of the pH, the reaction mixture was carefully adjusted to neutrality, and the reaction (activated ester → nitroxyl amide)[21] was continued for approximately 2 days. The labeled cell wall matrices were washed extensively with 60% EtOH:H_2O and subsequently dehydrated with absolute EtOH. The cell wall materials were stored in absolute EtOH until critical point dried. Poly(galacturonic acid) (H^+ form; PGA) nitroxyl amide spin-labeling reactions were performed in aqueous solution as described previously.[8]

H_2O and Ca^{2+} Exchange. For the hydration experiments, intact critical point dried cell wall and PGA powders were packed into open-ended 2-mm-i.d. quartz tubes, carefully weighed and equilibrated in a 100% relative humidity chamber. The level of hydration was monitored gravimetrically as a function of time; at each time interval, an EPR spectrum was recorded. Moistened cotton plugs were kept inside the EPR tubes to maintain that particular level of hydration. In order to clarify the hydration process, we have provided data (Figure 2) from which both the number (N) and electron–nuclear distance (r) of nitroxyl amide bound ^2H_2O can be determined on spin-labeled macromolecules. These data were obtained at 4.2 K using a 3-pulse electron spin-echo modulation (ESE) pulse sequence[22] on moderately (Figure 2A; 30% [w/w] ^2H_2O) and fully hydrated (Figure 2B; ≥50% [w/w] ^2H_2O) nitroxyl amides of a model homopolygalacturonan. Simulations of the ESE modulation envelopes indicate that up to 4 and 8 water molecules (parts A and B of Figure 2, respectively) bind equivalently to each nitroxyl moiety at approximately 3.6 Å with an isotropic coupling (A_{iso}) of 0.0 MHz. The computer simulation of these ESE envelopes was problematic since there was a possibility of spectral distortion of the initial part of the time domain array due to an inner layer of bound ^2H_2O with smaller r values and a nonzero A_{iso}. These data do, however, provide a relative measure of nitroxyl near-neighbor water binding. Figure 3 shows the approach to equilibrium hydration of plant cell wall matrices as a function of time in a saturated relative humidity chamber. The level of hydration at or near equilibrium (200 h or more of hydration) was approximately 100% [w/w].

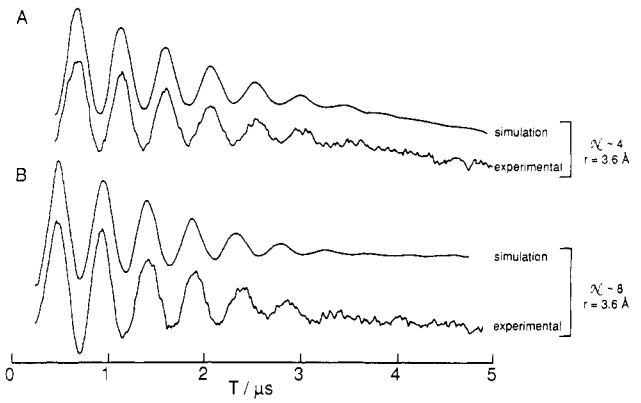

Figure 2. Three-pulse electron spin–echo modulations of partially hydrated (^2H_2O) PGA nitroxyl amides at 4.2 K. Time domain modulation envelope A is a result from a moderately (ca. 30% [w/w]) hydrated matrix; modulation envelope B is from a fully (ca. 100% [w/v]) hydrated matrix. The time between the first two pulses was 0.28 μs.

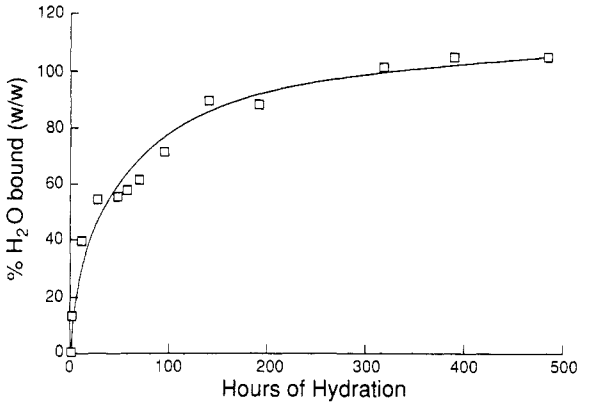

Figure 3. Dependence of polymer hydration on time in a 100% relative humidity chamber.

Nitroxyl amide (~2 × 10^{19} spins/g) labeled cell walls were equilibrated in 10.0 mL of 50–400 mM $CaCl_2$ in 60% EtOH:H_2O at room temperature overnight, washed extensively with 60% EtOH, dehydrated in absolute EtOH, and critical point dried. Twenty microliters of 1% [w/v] nitroxyl-labeled PGA solutions were injection precipitated into 10.0 mL of 60% EtOH:H_2O solution with 0.05–2 M $CaCl_2$. These samples were treated the same way as the labeled cell wall material. The Ca^{2+}-exchanged PGA samples were powdered after drying. Ca^{2+} levels for all samples

were measured by utilizing standard atomic absorption spectrophotometric techniques.

Spectroscopic Measurements. EPR measurements were made with a Varian E-109B X-band spectrometer interfaced with an IBM 9000 computer. (*Reference to brand or firm name does not constitute endorsement by the U.S. Department of Agriculture over others of a similar nature not mentioned*). Variable-temperature EPR experiments were performed by using a Varian E-257 variable temperature accessory; the temperature measurement error was found to be approximately ±0.5 K. Temperature control was carried out by circulating cold N_2(g), obtained by heating N_2(l), through the EPR cavity via a flow Dewar. For the variable-temperature studies, hydrated samples were placed in the spectrometer only after 97 K was reached in order to prevent dehydration. The z axis component of the **A** tensor (A_z) anisotropy was measured by calibration against the 87.3-G hyperfine splitting of dilute Mn^{2+} doped in a MgO matrix. The number of nitroxyl spins was calculated against a platelike Cr^{3+}/Al_2O_3 crystal (11.38×10^{15} spins). Computer simulations[23] of the rigid limit were used to fit with 77 K empirical EPR spectra on a Modcomp Classic 16-bit computer.

Cross-polarization and magic angle sample spinning (CPMAS) NMR spectra were obtained at a ^{13}C frequency of ca. 15 MHz on a JEOL FX-60QS spectrometer with a ^1H decoupling field strength of 11 G. One-thousand twenty-four data points were sampled and zero filled to 4096 for data acquisition. All chemical shifts were assigned relative to hexamethylbenzene's (HMB) methyl resonance (δ = 17.36 ppm) based on the position of Me_4Si. Primary plant cell wall samples (300–500 mg of dry weight) were spun (2.4 kHz) at the magic angle (54.7°) in a Kel-F bullet rotor; the angle was set with HMB prior to each experiment. NMR experiments were performed in the presence of dry N_2(g) flow. Spectra utilized in this work were acquired with 0.8 ms of ^1H–^{13}C thermal contact.[16]

Results

The sugar acid containing macromolecules of intact higher plant cell walls are presumed to be located in a highly diverse microenvironment. The homopolygalacturonans are only one, albeit major, portion of the pectic polysaccharides within the cell wall matrix, which, in turn, are surrounded by other complex heteropolymers such as hemicellulose. In this work, we have begun to further probe certain weak intermolecular forces (e.g., Ca^{2+}-induced cross-linking) by specifically cleaving methyl ester blocks on the sugar acid matrix as well as removing other near-neighbor polysaccharides that are believed to interact with the sugar acid matrix via hydrogen bonding. By performing such treatments, we hope to liberate enough nitroxyl amide motion in order to facilitate the study of Ca^{2+}-induced motional perturbations in both the dry and hydrated solid states.

Rotational Motions in the Dehydrated State. CPMAS NMR spectra[24] obtained from dehydrated nitroxyl amide labeled wall samples (Figure 4B) display a high degree of methyl ester ($\delta \cong 54$ ppm) line broadening even though only about 6% (2×10^{19} spins/g) of the available carboxyl groups has been labeled. This broadening effect was completely reversible upon reducing the nitroxyl (N–O•, Figure 4B) to the hydroxyl amide (N–OH, Figure 4A) with ascorbate. This result argues that the nitroxyl amides attach relatively close (e.g., ≤100 Å) to the methyl ester domains, which could restrict nitroxyl amide rotational freedom. Specific esterase (PME) treatments were performed to remove these domains from the sugar acid matrix. CPMAS NMR spectra of the control and PME-treated cell walls (without spin labels) are shown in parts A and B of Figure 5, respectively. These spectra demonstrate that the methyl esters were selectively removed from the cell wall matrix since the 54 ppm resonance disappears without a concomitant change in the relative areas of the anomeric or carbonyl resonances. Both control and

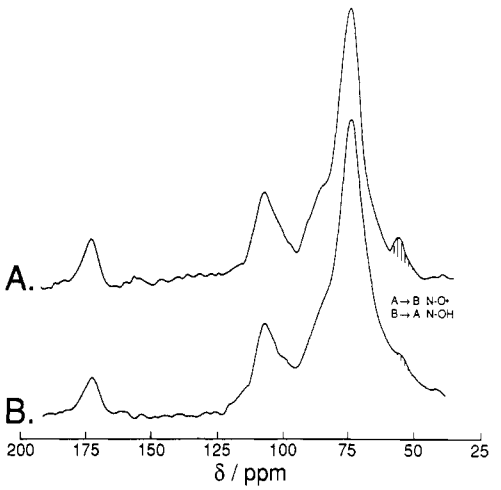

Figure 4. CPMAS NMR spectra of a higher plant cell wall matrix (0.8 ms of ^1H-^{13}C thermal contact) obtained using 10000 transients (A) or 40000 transients (B) with recycle time of ca. 2 s. Spectrum A represents a control experiment (no nitroxyl amide). Spectrum B is the same as A but with the free acid reacted[17] with 4-amino-2,2,6,6-tetramethylpiperidinyl-1-oxyl to form the amide (ca. 2×10^{19} spins/g). Upon reduction of the nitroxyl group with ascorbate, B reverts to A.

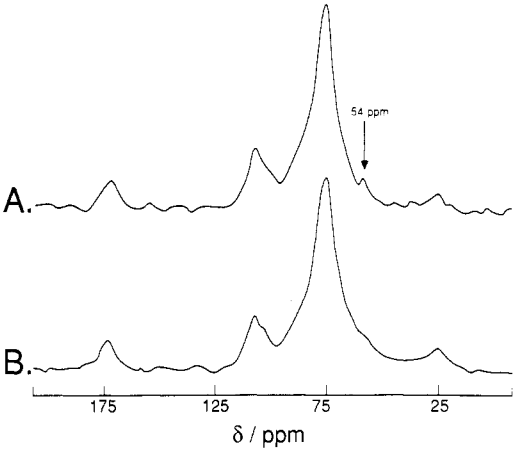

Figure 5. CPMAS NMR spectra of a higher plant cell wall matrix (0.8 ms of ^1H–^{13}C thermal contact) obtained using 40000 transients with a recycle time of ca. 2 s. Spectrum A represents the PME control experiment (e.g., same as the PME treatment but without the enzyme). Spectrum B represents the PME treatment.

PME-treated cell walls were subsequently spin labeled.

Nitroxyl amide EPR experimental line shapes for the labeled cell walls at 77 K were calculated using a rigid limit simulation program.[23] The nitroxyl simulations (Figure 6C,D) match well with the experimental spectra (Figure 6A,B), suggesting that, despite the heterogeneous nature of the cell wall matrix, the signals were averaged out similar to the calculated spectra. Both control and PME-treated cell wall samples had about 2.5×10^{19} nitroxyl amide spins/g of cell wall. Assuming the average degree of polymerization was about 83,[25] one carboxyl group was labeled for about every one homopolygalacturonan block and is evidence that there was no spin–spin broadening contributing to the nitroxyl amide's line shape. Spectroscopic parameters derived from the best fit simulations are listed in Table I. The principal components of the **g** and **A** tensors from control and PME-treated cell walls were made slightly different in order to more closely fit the intensity of the middle hyperfine component (I = 0) of the total nitroxyl spin to the experimental spectra. The simulated spectra of the PME-treated cell wall exhibited larger g_x's, g_y's, and line widths than that of the control, suggesting

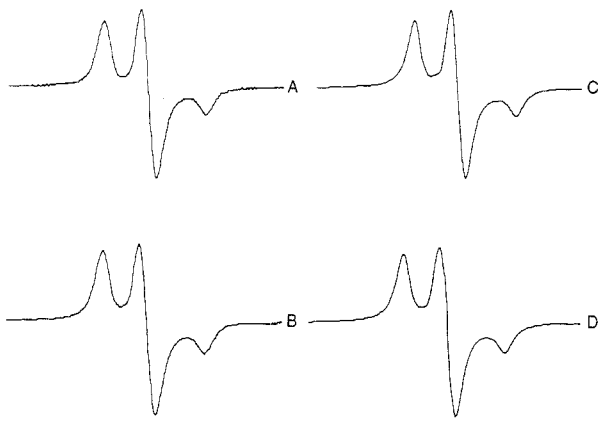

Figure 6. Experimental EPR spectra obtained at 77 K of (A) control and (B) PME-treated cell wall matrices. Best fit simulated spectra[23] for A and B are shown in C and D, respectively. The magnetic parameters for the simulated spectra are described in Table I.

Table I
Paramagnetic Parameters from the Best Simulations That Fit the Control and PME-Treated Nitroxyl Amide Labeled Cell Wall Homopolygalacturonans Using a Rigid Limit Program[a,23]

	cell walls		
parameter	control	PME	PGA
g_x	2.0095	2.0098	2.0095
g_y	2.0068	2.0060	2.0059
g_z	2.0022	2.0022	2.0022
A_x/G	7.0	7.0	7.0
A_y/G	4.5	4.5	4.5
A_z/G	36.36	36.36	35.8
α	7.0	7.5	5.8
β	0.2	0.3	0.2

[a] The orientation-dependent line width parameters are designated as α and β, from the equation, $1/T_2 = \alpha + \beta \cos^2 \theta$, where θ is the polar angle relative to the z magnetic axis (Figure 1) of the nitroxyl amide.

an altered, relative to the control, conformation of the sugar acid domains. Atomic absorption analysis of both cell wall treatments indicated that very low levels of Ca^{2+} (0.15–0.2% of available sites filled) were bound; this finding argues that the observed line shape differences were not due to variable levels of Ca^{2+}.

EPR spectra of the dehydrated/spin-labeled control and PME-treated cell walls were obtained at 98–358 K. In previous work,[8] we found that when an empirical relation was used (eq 1)[26] the obtained correlation times at low temperatures (160–233 K) were somewhat higher than those from detailed line shape simulations using stochastic Liouville theory.[27] In the present system, even though EPR powder patterns of the cell walls had larger values of A_z than that of PGA, we still considered the **A** tensors to have relatively low anisotropy. Because of this, we used an empirical formula to estimate rotational correlation times, τ_R, as follows:

$$\tau_R = a\{1 - S\}^b \quad (1)$$

whereupon a and b are constants for different models listed in Table II, and S is the ratio of the separation of the outer extrema ($2A_z$) of a given spectrum at some temperature to that of the rigid limit. From previous work,[8] using detailed line shape simulations,[27] the moderate jump diffusion model was determined to fit best for correlation times observed in the low-temperature range. We also have applied this model in calculating the correlation times at various temperatures in the cell wall system. The linear relationship between $\log_e (1/\tau_R)$ and reciprocal temperature over the range 98–158 K is shown in Figure 7. For both control (open circles) and PME-treated (closed circles) cell walls, the activation energies (E_a) for rotational motion were 0.60 and 1.26 kcal/mol, respectively. At these low temperatures, a small E_a was required for local motions, which we have interpreted[8] to be due to the reorientation of the nitroxyl group at the NH–C_1 bond (Figure 1). Arrhenius plots for the whole temperature range (98–358 K) clearly demonstrate a transition with two different E_a's.[8] The calculated activation energies for internal motions (rotation of the nitroxyl group around the main chain[8]) which occur at high temperatures (233–358 K) in the dehydrated state for PGA and cell walls are listed in Table II. These data (Figure 7, Table II) indicate that less activation energy was required for local and internal motions in the control than PME-treated cell wall matrices, suggesting that there were large differences in the higher order structure spatially close to the spin labels due to the methyl ester functionality alone. The internal motions of PGA, when treated in the same fashion as cell walls, required about the same E_a as PME-treated cell walls. Thus, internal motions in the control sample had a remarkably lower E_a than either PGA or PME-treated cell walls.

Table II
Activation Energies for Internal Motion between 233–358 K[a]

	E_a/kcal·mol^{-1}	
sample type	moderate-jump	Brownian diffusion
PGA	3.37	4.99
control	2.46	3.66
PME	3.57	5.30

[a] E_a's were calculated from the empirical formula,[26] $\tau_R = a(1 - S)^b$, where $a = 6.99 \times 10^{-10}$ and 2.57×10^{-10} and $b = -1.20$ and -1.78 for moderate-jump and Brownian diffusion models, respectively.

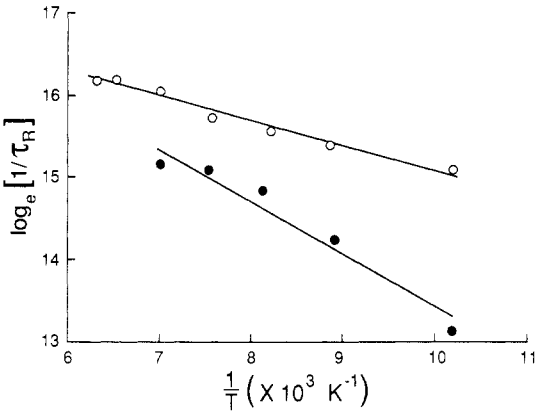

Figure 7. Arrhenius plots for local motions (98–158 K) in the control (open circles) and PME-treated (closed circles) higher plant cell wall matrices. Activation energies (E_a) were 0.60 and 1.26 kcal·mol^{-1}, respectively.

In order to elucidate the effect of Ca^{2+} on nitroxyl amide internal motions in dehydrated PGA as well as the native wall matrix, a series of activation energies were obtained using the moderate-jump diffusion model at different levels of Ca^{2+}_{bound} (Figure 8). There was a greater rate of E_a increase, as a function of increasing Ca^{2+}_{bound}, in PGA than there was in native primary plant cell walls. This observation indicates that Ca^{2+} cross-links more effectively, from the standpoint of the nitroxyl amide, in the more homogeneous macromolecule than in the native sugar acid matrix. However, we feel that this apparent discrepancy in Ca^{2+} effects on nitroxyl amide internal motion could be affected by the fact that the spin-label moieties may attach

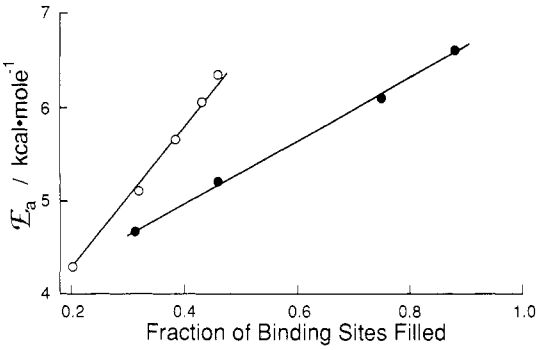

Figure 8. Internal motion E_a's (kcal·mol^{-1}) as a function of the fraction of binding sites filled with Ca^{2+} (moles of Ca^{2+}/{total moles of uronic acid/2}) for labeled PGA (open circles) as well as higher plant cell wall homopolygalacturonans (closed circles).

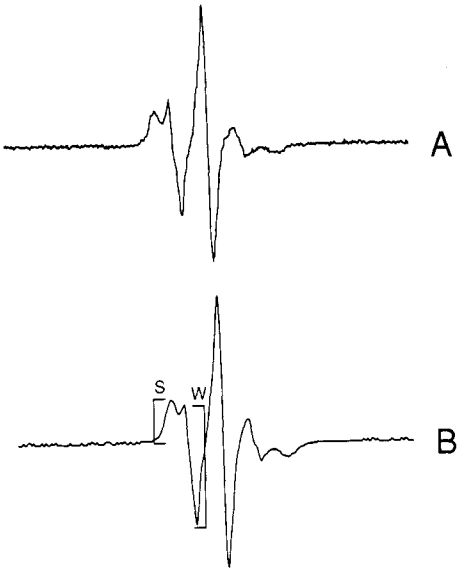

Figure 9. EPR spectra of nitroxyl amide labeled (A) PGA hydrated to the level 0.89 g of bound H_2O/g of PGA and (B) cell walls with 1.0 g of bound H_2O/g of solid.

spatially close (Figure 4) as an amide to the methyl ester blocks, which exist only in the native polymer lattice, thereby lessening the divalent cation's ability to influence the nitroxyl amide's motion. Indeed, the lower activation energies for the native cell wall with the same Ca^{2+} level as PGA argue that the nitroxyl spin labels are providing spatially specific information on Ca^{2+} effects at or near cell wall methyl ester domains.

Motions in the Hydrated State. In the hydrated solid state, the higher order structure of cell wall matrix homopolygalacturonans is modulated by bound water molecules.[28] Knowledge about the spatial deformations, as measured by different molecular flexibilities, upon hydration may assist in the elucidation of the higher order structure of these sugar acid containing matrix polysaccharides. EPR spectra of spin-labeled PGA and cell walls under similar conditions of hydration are shown in parts A and B of Figure 9, respectively. The overlapped signals of the isotropic (weakly immobilized, W) and anisotropic components (strongly immobilized, S) were identified to be from at least two domains, which were previously interpreted[8] to result from localized disruptions of the ordered matrix. Upon equilbrium hydration, the weakly immobilized components of PGA (0.89 g of H_2O/g of PGA, Figure 9A) exhibited faster motion than that of the cell walls (ca. 1.0 of g H_2O/g of cell walls, Figure 9B).

EPR spectra of fully hydrated control and PME-treated cell wall matrices with increasing levels of bound water are

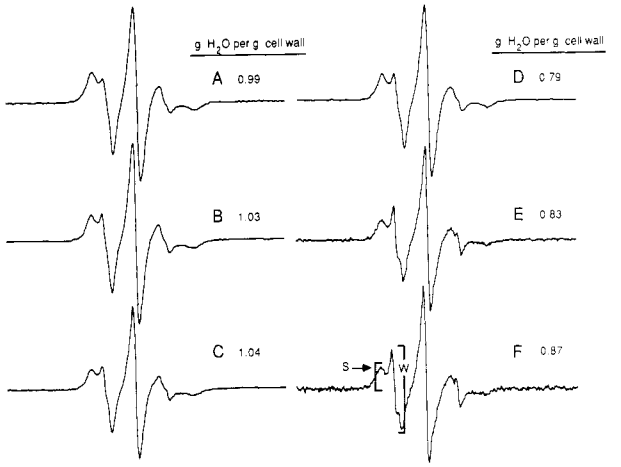

Figure 10. Hydration dependence of spin-labeled (A–C) control and (D–F) PME-treated cell wall matrices on EPR line shape. The ratio, W/S, is defined for spectrum F.

shown in parts A–C and D,E of Figure 10, respectively. The weakly immobilized components (W) of the cell walls lacking the methyl ester domains were well resolved (e.g., compare A and F of Figure 10). As the level of hydration increased, the W/S ratio of spectra in Figure 10 gradually increased, indicating that the population of weakly immobilized components grew. The detection of the signal from the weakly immobilized label was shown[8] to be indicative of changes in the cell wall homopolygalacutonan's microenvironment due to weaker interactions with other polymers in the matrix. Because of this, we have used the intensity ratio of weakly and strongly immobilized signals, designated as W/S, as a useful parameter to monitor relative changes in spin populations in the ordered domains. For example, comparing parts A and F of Figure 10, the W/S ratio for the control and PME-treated cell walls (0.99 and 0.87 g of H_2O/g of cell wall, respectively) was 2.49 and 3.69, suggesting that there was a larger population of spins with less motional hindrance in the deesterified wall matrix even when the level of bound water was less than that of the control. We therefore hypothesize that the methyl ester steric and interchain hydrophobic interaction effects on the label's motion, due to their spatial proximity, account for the increase in the nitroxyl amide's rotational freedom upon demethylation.

Alkali has been the classical chemical method for removing hemicellulose, which is presumably hydrogen bonded to cellulose, from the cell wall.[20] Unfortunately, such a treatment can also break other types of bonds such as glycosidic linkages (via β elimination[9]) and can hydrolyze methyl esters and acetylated groups as well as modify ionic bonds such as calcium bridges. The CPMAS NMR spectrum of a 2 N KOH extracted cell wall matrix (Figure 5B) displayed the loss of the methyl ester's 54 ppm resonance, indicating that these functionalities were removed concomitant with the β-D-glucans of hemicellulose. Since the alkali treatment was performed at room temperature and the β-elimination or transelimination process is most efficient with the addition of heat,[9] we have assumed that the most significant effect of the KOH treatment would be the removal of hemicellulose from the wall lattice as well as the saponification of the methyl ester functional groups. The spin-labeling reaction was performed after the alkali treatment and EPR spectra were acquired at 77 K. The alkali-treated cell wall EPR spectra exhibited a z-axis hyperfine coupling, A_z, of 36.79 G, which was considerably larger than the A_z for cell walls without the alkali treatment (Table I). When the nitroxyl amide labeled alkali-treated cell wall sample was hydrated to 0.85 g of

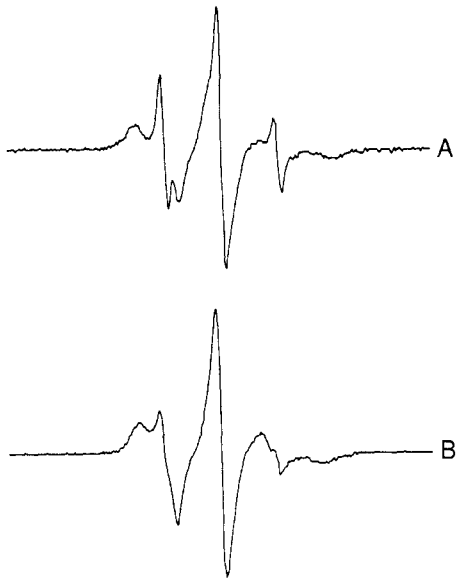

Figure 11. EPR spectrum (A) of labeled cell walls treated with 2 N KOH and fully hydrated to 0.85 g of bound H_2O/g of cell walls. EPR spectrum (B) of a Ca^{2+}-doped sample A (0.88 Ca^{2+} per binding site) and hydrated to a level of 1.1 g of H_2O/g of solid.

H_2O/g of cell wall and the EPR spectrum measured (Figure 11A; W/S = 5.03), the W/S ratio was much larger than the specifically deesterified (PME-treated) cell wall matrix (Figure 10E; W/S = 3.61) with a comparable level of hydration. The larger value of W/S in the hemicellulose-removed (and demethylated) wall matrix relative to that of the specifically deesterified cell walls indicates that there was an increase in the rotational freedom of the nitroxyl labels by the partial removal of hemicellulose alone. These results suggest that portions of the hemicellulose matrix must be spatially close to the labeled homopolygalacturonan chains. Upon treatment of the hemicellulose-removed cell walls with Ca^{2+} (0.88 cations per binding site; Figure 11B), the W/S ratio was observed to decrease from 5.0 (Figure 11A) to 3.6 (Figure 11B). This change in the population of weakly immobilized components as a function of bound Ca^{2+} indicates that the W/S parameter is a reasonable measure of the spin label's rotational freedom.

More specifically, it is of interest to perform similar studies to those above with respect to perturbations of cell wall homopolygalacturonan segmental motion in the hydrated solid state. The hyperfine splitting ($2A_z$) of the strongly immobilized component in the EPR spectral envelope decreased drastically between 220 and 250 K. A weakly immobilized component started to appear at ca. 260 K and increased in intensity at a higher temperature. The EPR spectra recorded at temperatures higher than 260 K displayed an increasing fraction of weakly immobilized components, and therefore, it was difficult to extract their intrinsic line shapes; because of this, segmental motion in temperatures greater than 260 K was not investigated. Figure 12 shows the Arrhenius plots of fully hydrated (ca. 1.0 g of H_2O/g of cell wall) control cell walls (with ca. 0.02 Ca^{2+}_{bound} per site) over the temperature range 183–263 K. Correlation times for segmental motion were obtained by using both the moderate-jump (Figure 12, open circles) and Brownian diffusion (Figure 12, closed circles) models. The obtained energies of activation were approximately 3–4 kcal/mol, which were much smaller than E_a's for the PGA model system (6.5–9.6 kcal/mol)[8] shown previously. A similar finding was noted in the dry cell wall powders in which internal motions required less E_a than did PGA with the same level of Ca^{2+} (Figure 7).

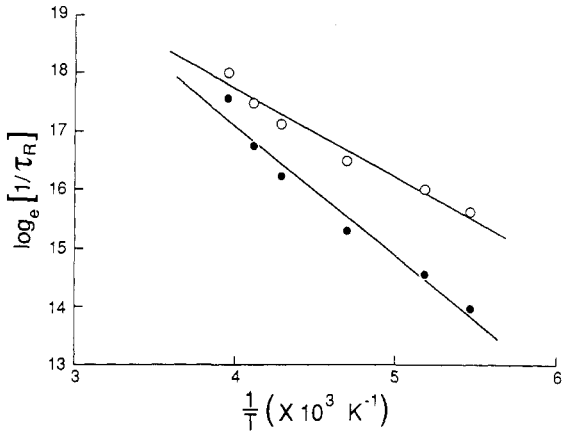

Figure 12. Arrhenius plots of fully hydrated higher plant cell wall matrices (183–263 K) using moderate-jump and Brownian diffusion models of motion. E_a's were 2.97 and 4.42 kcal·mol^{-1}, respectively.

These data indicate that the strongly immobilized regions of cell wall sugar acid domains are more flexible than equivalent loci in the PGA model system. These findings are not surprising considering that other data (Figures 4 and 8) indicate that the spin labeles selectively attach to free acid regions near the methyl ester domains and, in turn, are less affected by weak intermolecular coupling, thereby displaying diminished E_a's.

As shown before,[8] upon hydration, the behavior of these macromolecules can be more extensively investigated when examined with respect to the diffusion of water bound to the hydrated cell wall's polymer matrix. From parts A and B of Figure 10, we found that (1) the strongly immobilized component's $2A_z$ narrows and (2) the weakly immobilized nitroxyl amide population increases upon increasing the level of hydration; the latter finding is evidenced by the W/S ratio increasing as a function of bound water (Figure 10). In order to analyze the available data, we have modified the Fujita–Doolittle equation[29–32] as follows:

$$\Xi = -\frac{1}{\log_e [\tau_R/\tau_R^{ref}]} = -\frac{1}{\log_e [\{W/S\}_{ref}/\{W/S\}]} = f_2 + \left\{\frac{f_2^2}{v_1\zeta}\right\} \quad (2)$$

$$\lim_{v_1 \to v_{max}} \Xi = f_2 \quad (3)$$

whereupon there is a collapse of the apparent free volume of the polymer matrix upon saturation or equilibrium hydration (e.g., as v_1 approaches v_{max}; the volume fraction of the diluent, v_1, is equivalent to the degree of hydration in units of grams of H_2O/gram of solid). The terms f_2 and ζ are constants for a given polymer–diluent system corresponding to the free volume fraction in the reference state and the proportionality constant for the dependence of the total fractional free volume, f_1, on the diluent volume fraction (e.g., $f_1 = \zeta[v_1 - v_1^{ref}] + f_2$; v_1^{ref} is the diluent volume fraction in the dehydrated state and is assumed to be zero). In this work, we have introduced the W/S ratio (room temperature) to eq 2 since we know that, for a decrease in correlation time (faster motion), there is a corresponding increase of the weakly immobilized population or W/S ratio. ζ can be obtained once the intercept and slope of a plot of $-1/\log_e [\{W/S\}_{ref}/\{W/S\}]$ versus the reciprocal of v_1 (eq 2) is known (Figure 13). The linearity of the plots in Figure 13 indicates that the W/S ratios, relative to the reference or dehydrated state, are good measures of the rotational diffusion of the nitroxyl amide labels, which, in

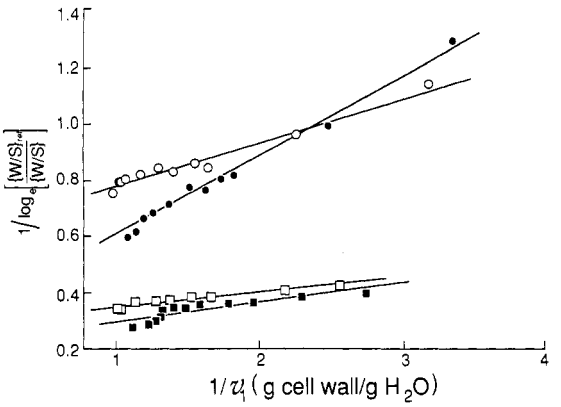

Figure 13. Fujita–Doolittle plots based on eq 2 in control cell walls (open circles) with coupling constant $\zeta = 1.74$; PME-treated cell walls (closed circles) with $\zeta = 0.72$; PGA with 0.11 Ca^{2+} bound per site (open squares) with $\zeta = 0.38$; PGA with 0.32 Ca^{2+} bound per site (close squares) with $\zeta = 2.40$.

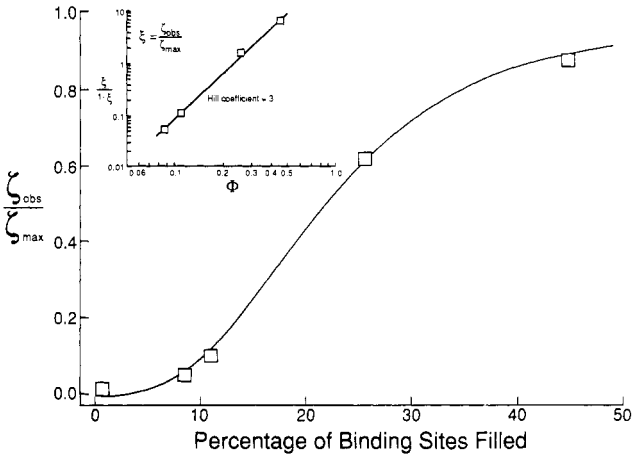

Figure 14. Dependence of PGA ξ_{obs}/ξ_{max} on the percentage of Ca^{2+} binding sites filled (e.g., 100Φ). The curve is the best fit to eq 4 whereupon $n = 2.98 \pm 0.15$. Inset figure: Hill plot (eq 6) for these same data.

turn, correlate[8] with the monomeric translation diffusion coefficient of the diluent which is bound to the polymer.

In Figure 13, the control and PME-treated cell walls (open and closed circles, respectively) gave ζ's of 1.74 and 0.72, respectively. As a comparison, similar plots for PGA (0.11 and 0.32 Ca^{2+} per binding site are represented by open and closed squares, respectively) are also shown. There was a dramatic increase in ζ from 0.38 to 2.35 for PGA samples with levels of ca. 11% or 32% binding sites filled with Ca ions, respectively. These experiments are evidence that ζ is a measure of the intermolecular coupling of the labeled matrix with its surroundings. ζ's for the specifically demethylated cell wall homopolygalacturonans were about 58% lower than ζ's for untreated walls. The experiments depicted in Figure 13 also demonstrate that the deesterified matrix had a 2-fold larger intermolecular coupling constant (ζ) than that of the 11% Ca^{2+} salt of PGA. The latter observation is not surprising since homopolygalacturonan blocks in the wall network are known to be much larger[24] and more complex and therefore should have a greater degree of intermolecular coupling with near-neighbor matrix polysaccharides. In order to further study the cross-linking effect of Ca^{2+}_{bound} on homopolygalacturonan motion, we chose to work with the PGA system. EPR spectra were obtained at room temperature with various levels of hydration as a function of Ca^{2+}_{bound}. The coupling constants obtained from eq 2 are shown in Figure 14. ζ's increased with increasing the percentage of Ca^{2+} bound, on an available site basis, and tend to saturate ($\zeta_{max} \cong 4$) at approximately 0.5 bound Ca ion per site. In these studies, we have assumed that the intermolecular coupling parameter would display typical saturation behavior (e.g., as shown for water binding to the cell wall matrix in Figure 3) with respect to the fraction (Φ) of binding sites filled with Ca^{2+}. To test this idea, we have modified the Hill equation as follows:

$$\xi = \frac{\zeta_{obs}}{\zeta_{max}} = \frac{K\Phi^n}{1 + K\Phi^n} \tag{4}$$

$$\frac{\xi}{1 - \xi} = K\Phi^n \tag{5}$$

$$\log\left\{\frac{\xi}{1 - \xi}\right\} = \log K + n \log \Phi \tag{6}$$

whereupon ζ_{max} was estimated to be approximately 4, K is an arbitrary constant, and n, the Hill coefficient, is a measure of a system's cooperativity at equilibrium. The best fit curve for eq 4 is shown in Figure 14 ($n = 2.98 \pm 0.15$). In normal usage, ξ would be treated as the fractional saturation ($\bar{\alpha}$) of an ensemble of binding sites on a macromolecule, Φ as the total initial concentration (activity = $\mathcal{A}_L$) of the ligand and K as an average equilibrium constant. However, if ζ is a parameter sensitive to the spatial organization of the Ca^{2+} cross-linkages in the polyuronic acid matrix, then its behavior with respect to Φ, the fraction of sites filled with Ca^{2+}, should be similar to $\bar{\alpha}$ as a function of $\mathcal{A}_L$ in a cooperative Ca^{2+}-binding system such as the homopolygalacturonans.[15,16,28] Because of this latter principle, a plot of $\log\{\xi/(1 - \xi)\}$ versus $\log \Phi$ (Figure 14, inset) should be linear and the slope equal to n, which, in turn, should be much larger than unity. For these data, n was approximately 3. Such behavior argues that ζ is a parameter that describes the spatial distribution of the Ca^{2+} cross-linkages; thus, if $n \sim 1$, the distribution is random, whereas if n is much larger than 1 the cations are distributed in a spatially nonrandom or sequential fashion as has been proposed before.[15,28] These data indicate that the Fujita–Doolittle relationship (eq 2) can be applied to these systems when characterizing perturbations induced by weak intermolecular forces, such as the Ca^{2+} bridges, on a hydration deformed sugar acid polysaccharide system.

Discussion

The Dry Solid State. Rigid-limit powder pattern EPR spectra of nitroxyl amide labeled cell walls and their simulated spectra (Figure 6) suggest that labeled homopolygalacturonan blocks in the cell walls exhibit larger hyperfine splitting along the magnetic z axis than that of PGA (see Table I), which is evidence that the microenvironment around the nitroxyl labels was more anisotropic. The labels could be in a more crystalline region than that of the model compound. The larger line width of cell wall nitroxyl amides over those for PGA is probably due to a broader spatial distribution of the various nitroxyl sites. The differences in g values between the control and PME-treated cell walls are small, but one could argue for a slightly larger **g** tensor anisotropy in the specifically demethylated wall matrix.

The E_a's (Figure 6 and Table II) for local (98–158 K) and internal (173–358 K) motion of the spin labels are greater in their native state than upon deesterification. These data, in conjunction with Figure 4, argue that the nitroxyl amine spin labels selectively favor reaction with carboxyl functional groups, to form the amide, in domains spatially close to hydrophobic methyl ester groups which, in turn,

break up the ordered matrix. Thus, by deesterification, we have increased the charge density in the uronosidic domains which could cause a dissociation of like polymer chains due to ionic repulsion and result in a more amorphous matrix. The larger line width of the PME-treated cell walls, relative to that of the control, could be due to inhomogeneous broadening, which results from a larger number of magnetically nonequivalent nitroxyl amide sites. Our results (Figure 7 and Table II) in solid dehydrated states on demethylated and control cell wall sugar acid polymers are supported by NMR studies[33] where it was suggested that the effect of side-group substitution is to lower the temperature at which chain axis rotation is observed in the crystalline phase. Our results (Table II) for E_a's in the dehydrated solid state support these conclusions and strengthen our hypothesis that the nitroxyl labeled homopolygalacturonan chains are in a crystalline region spatially close to the methyl ester functional groups. These data also support the hypothesis that the matrix or non-cellulosic polysaccharides have an oriented structure as suggested by Preston[34] and Senda.[35,36] In the amorphous phase, it has been shown that bulky side groups provide an energetic barrier to local motion; however, our results with cell walls indicate that the E_a's for motions were less when methyl esters were the substituent. These findings suggest that the methyl esters deform the main homopolygalacturonan chains enough to contribute in the formation of a crystalline phase. Upon removing the methyl esters from the matrix, the conformation changes and the overall structure becomes more amorphous, thus elevating the energy required for internal motions. In order to retain this crystalline structure, the methyl ester domain must exist, at least in part, in a regular pattern and agrees with recent findings[24,28] which indicate that the methyl ester domains in higher plant cell wall matrices exist as a spatially sequential array.

In order to explore in greater detail the structural differences, relative to the bonded spin label, between our known sample, PGA, and equivalent moieties in higher plant cell walls, we performed an experiment (Figure 8) that indicated that an increase in the E_a's for τ_R, with respect to bound Ca^{2+}, in cell wall homopolygalacturonans was slower than similar observations for the model system. This finding implies that the internal motion of the labeled chains in the cell walls was not as sensitive to ionically bonded Ca^{2+} as the model compound. PGA is a nonesterified homopolymer lacking rhamnosyl and other neutral sugar residues. The intermolecular forces within a Ca^{2+}–PGA matrix are mainly ionic. On the other hand, homopolygalacturonan blocks in plant cell walls are only a part of a larger heteropolymer system of unknown molecular weight, which contains up to 20–30% neutral polysaccharides. Rhamnogalacturonan residues have been proposed to link directly to chains of neutral sugar,[37] which could contribute to the interaction of nitoxyl amides with near-neighbor neutral residues and therefore result in lower motional E_a's. Even though our data (Figures 4 and 10) argue that our spin labels selectively attach spatially near the methyl ester domains, the galacturonan-containing wall polymers show no competitive inhibition of matrix interchain association in the presence of Ca^{2+}. This is attributed to the fact that the activation energy for internal motions in the plant cell walls, like the PGA system, gradually increases as a function of bound Ca^{2+} in a linear fashion. There has been evidence[1,20,28,38] that Ca ions induce association of homopolygalacturonan blocks within pectin into aggregates. Our data seem to indicate that these Ca^{2+}-induced aggregates are, energetically speaking, highly stabilized in the cell wall matrix. We also noticed that the presence of bound Ca ions did not induce any significant line broadening. This is because the divalent cations are bound in a spatially sequential fashion at a distance $\geq$10 Å,[15,28] which is the marginal distance limit for nitroxide–metal ion interaction sensitivity.[39] In order to effectively investigate the conformational flexibility of nitroxyl amide labeled cell wall homopolygalacturonans as a function of weak intermolecular forces, hydration was introduced to the system so that perturbations in the distribution of the labels with restricted motions and, hence, the cross-linking density due to Ca^{2+} bridging could be measured more effectively.

Hydrated Solid States. Upon equilibrium hydration (Figure 3), it was estimated that there were 10–11 H_2O molecules bound to each sugar monomer unit in the wall matrix; of course, more H_2O molecules were associated with the nitroxyl amide residues (Figure 2). EPR nitroxyl amide spectra of a hydrated cell wall matrix showed an increasing population of weakly immobilized or isotropic components as a function of hydration; this was even more apparent in the enzymatically deesterified wall lattice (parts C and F of Figure 10), which suggests that greater rotational freedom was released upon removal of the methyl ester domains. The two main populations of nitroxyl spins[8] result from a strongly immobilized component from highly aggregated, possibly helical, domains and from isolated blocks with greater segmental motion, which result from localized disruption of the ordered matrix. In the cell wall system, we observed that the population of weakly immobilized components increased in size slower than that for PGA. The expanding population of isotropic components was found to be related to free volume theory (eq 2; Figure 13) since plots of $-1/\log_e [\{W/S\}_{ref}/\{W/S\}]$ versus the reciprocal of v_1 were linear. Thus, according to free volume theory, the average distance between homopolygalacturonan chains would increase upon hydration and result in a greater free volume and, consequently, more nitroxyl amide rotational freedom. Therefore, the accessibility of water diffusion through the polymer matrix, which is related to the motion of the spin labels,[8] can be monitored and one can obtain, quantitatively, an intermolecular coupling parameter, ζ, as described by the modified Fujita–Doolittle relation (eq 2). ζ's were reduced 58% when methyl ester groups were enzymatically removed from native cell walls. PGA's ζ was found to be at least 47% less than ζ of enzymatically demethylated cell walls. These results in the hydrated state were similar to those found for pectin molecules in solutions as visualized by electron microscopy.[40] In these studies, pectin microfibrils were observed to disperse after increasing the charge density via enzymic deesterification; unfortuantely, sample preparation for electron microscopy requires at least some dehydration since the experiments must be performed in a high vacuum. The smaller ζ for the demethylated cell walls suggest a weaker interchain linkage and, hence, weaker gel strength, which is known to occur in Ca^{2+}–pectate gels upon deesterification.[41,42] The rate of gelation[43] of pectinic acid has been shown to be controlled by the formation of hydrophobic interactions between methyl ester blocks. Our data support the behavior described in these studies of gelation in model systems and emphasize the important role methyl ester functional groups play in maintaining the structural integrity of plant cell wall matrices.

The effect of Ca^{2+} bridges was monitored by obtaining EPR spectra of a series of hydrated Ca^{2+} salts of PGA. The intermolecular coupling constants, ζ, obtained from

the slopes of the least-squares Fujita–Doolittle plots were found to be a direct measure of the Ca^{2+}-induced loss of deformability in the hydrated homopolygalacturonan chains. The increase in ζ (Figure 14) with level of bound Ca^{2+} indicated that there was a reduction in the deformability of the wall's matrix polysaccharide network since Ca^{2+} replaces some bound H_2O molecules and forms ionic bridges with the free carboxylic acids. The tendency to saturate with respect to ζ at about 0.5 Ca ion bound per site suggests that a bound-ion-dependent conformational change in the polyanionic matrix occurs. This conclusion is supported by the fact that divalent cationic cross-linkages between adjacent homopolygalacturonan blocks displayed a positively cooperative effect on ζ as the fraction of binding sites being filled with Ca^{2+} increased. Such a bound-Ca^{2+}-dependent conformational perturbation would be expected for a cooperative ion-binding species[15] and supports circular dichroism work by Rees and co-workers,[38] for solutions, where there was shown to be a conformational change from the 3_1 to 2_1 helical structure in the transition from the dehydrated solid to gel phase.

From this work, the relative strength of various molecular constraints affecting a given sequence or block of a complex cell wall matrix polysaccharide due to localized steric (methyl ester domains) and cross-linking (due to Ca^{2+}) effects has been shown to be reasonably well represented by ζ, which can be obtained from modified Fujita–Doolittle plots. Other, more complicated, methods have been extensively discussed by several workers,[44,45] and the degree of intermolecular coupling has been estimated in several systems.[46,47] Using the fraction of mobile to rigid phase components (e.g., the W/S ratio) as a measure of the cross-link density has proved to give reasonable results in a complex system such as intact plant cell wall homopolygalacturonans. Our analysis was found to be similar to a method[48] for estimating the relative stiffness of molecular chains in polyelectrolytes whereupon the slope of plots of intrinsic viscosity versus reciprocal square root of the ionic strength was used as a measure of the relative stiffness in different polymer chains.

Acknowledgment. We thank L. Sivieri, R. Boswell, T. Dobson, and M. Taylor for technical assistance. We would also like to acknowledge Drs. L. Kevan and D. Goldfarb of the Department of Chemistry, University of Houston, for assistance with the electron spin–echo experiments.

Registry No. Ca, 7440-70-2; polygalacturonan, 68943-61-3; pectin, 9000-69-5.

References and Notes

(1) Preston, R. D. *Annu. Rev. Plant Physiol.* **1979**, *30*, 55–78.
(2) Grant, G. T.; Morris, E. R.; Rees, D. A.; Smith, P. J. C.; Thom, D. *FEBS Lett.* **1973**, *32*, 195–198.
(3) Albersheim, P.; Muhlethaler, K.; Frey-Wyssling, A. *J. Biophys. Biochem. Cytol.* **1960**, *8*, 501–506.
(4) Knee, M.; Barley, I. M. *Recent Advances in the Biochemistry of Fruits and Vegetables*; Academic Press: London, 1981; pp 133–148.
(5) McNeil, M.; Darvill, A. G.; Fry, S. C.; Albersheim, P. *Annu. Rev. Biochem.* **1984**, *53*, 625–663.
(6) Rees, D. A.; Morris, E. R.; Thom, D.; Madden, J. K. *The Polysaccharides*; Academic Press: New York, 1982; pp 195–290.
(7) Dea, C. M. J.; Morris, E. R.; Rees, D. A.; Welsh, J.; Barnes, H. A.; Price, J. *Carbohydr. Res.* **1977**, *57*, 249–272.
(8) Chamulitrat, W.; Irwin, P. L.; Sivieri, L. M.; Schwartz, R. M. *Macromolecules* **1988**, *21*, 141–146.
(9) Barrett, A. J.; Northcote, D. H. *Biochem. J.* **1965**, *94*, 617–627.
(10) Ben-Arie, R.; Kislev, N. *Plant Physiol.* **1979**, *64*, 197–202.
(11) Stevens, B. J. H.; Selvendran, R. R. *Carbohydr. Res.* **1984**, *135*, 155–166.
(12) Perring, M. A.; Pearson, K. J. *J. Sci. Food Agric.* **1987**, *40*, 37–42.
(13) Rees, D. A.; Welsh E. J. *Angew. Chem., Int. Ed. Engl.* **1977**, *16*, 214–224.
(14) Thom, D.; Grant, G. T.; Morris, E. R.; Rees, D. A. *Carbohydr. Res.* **1982**, *100*, 29–42.
(15) Irwin, P. L.; Sevilla, M. D.; Shieh, J. J. *Biochim. Biophys. Acta* **1984**, *805*, 186–190.
(16) Irwin, P. L.; Gerasimowicz, W. V.; Pfeffer, P. E.; Fishman, M. *J. Agric. Food Chem.* **1985**, *33*, 1197–1201.
(17) Irwin, P. L.; Sevilla, M. D.; Osman, S. F. *Macromolecules* **1987**, *20*, 1222–1227.
(18) Irwin, P. L.; Pfeffer, P. E.; Gerasimowicz, W. V.; Pressey, R.; Sams, C. E. *Phytochemistry* **1984**, *23*, 2239–2242.
(19) Pressey, R.; Avants, J. K. *J. Food Biochem.* **1982**, *6*, 57–74.
(20) Fry, S. C. *Annu. Rev. Plant Physiol.* **1986**, *37*, 165–186.
(21) Taylor, R. L.; Conrad, H. E. *Biochemistry* **1972**, *11*, 1383–1388.
(22) Kevan, L., Schwartz, R. N., Eds. *Time Domain Electron Spin Resonance*; Wiley: New York, 1979; pp 279–341.
(23) Polnaszek, C. F. Ph.D. Thesis, Cornell University, Ithaca, NY, 1976.
(24) Irwin, P. L.; Sevilla, M. D.; Chamulitrat, W. *Biophys. J.* **1988**, *54*, 337–344.
(25) Fishman, M. L.; Pfeffer, P. E.; Barford, R. A.; Doner, L. W. *J. Agric. Food Chem.* **1984**, *32*, 372–378.
(26) Goldman, A. S.; Bruno, V. G.; Freed, H. J. *J. Phys. Chem.* **1972**, *76*, 1858–1860.
(27) Freed, J. H. *Spin Labelling: Theory and Applications*; Berliner, L. J., Ed.; Academic Press: New York, 1976; Vol. I, pp 195–290.
(28) Irwin, P. L.; Sevilla, M. D.; Stoudt, C. L. *Biochim. Biophys. Acta* **1985**, *842*, 76–83.
(29) Hiroshi, F.; Kishimoto, A. *J. Polym. Sci.* **1958**, *18*, 547–567.
(30) Kishimoto, A.; Hiroshi, F. *J. Polym. Sci.* **1958**, *18*, 569–585.
(31) Ferry, J. D. *Viscoelastic Properties of Polymers*, 3rd ed.; Wiley: New York, 1980; pp 486–496.
(32) Brown, I. M.; Sandreczki, T. C. *Macromolecules* **1985**, *18*, 2702–2709.
(33) Vega, A. J., English, A. D. *Macromolecules* **1980**, *13*, 1635–1647.
(34) Preston, R. D. *The Physical Biology of Plant Cell Walls*; Chapman and Hall: London, 1974; pp 187–191.
(35) Morikawa, H.; Senda, M. *Plant Cell Physiol.* **1978**, *19*, 327–336.
(36) Morikawa, H.; Hayashi, R.; Senda, M. *Plant Cell Physiol.* **1978**, *19*, 1151–1159.
(37) Chapman, H. D.; Morris, V. J.; Selvendran, R. R.; O'Neill, M. A. *Carbohydr. Res.* **1987**, *165*, 53–68.
(38) Morris, E. R.; Powell, D. A.; Gidley, M. J.; Ress, D. A. *J. Mol. Biol.* **1982**, *155*, 507–516.
(39) Berliner, L. J. *Molecular Motion in Polymers By ESR*; Boyer, R. F., Keinath, S. E., Eds.; Harwood Academic: New York, 1978; pp 15–17.
(40) Hanke, D. E.; Northcote, D. H. *Biopolymers* **1975**, *14*, 1–17.
(41) Powell, D. A.; Morris, E. R.; Gidley, M. J.; Rees, D. A. *J. Mol. Biol.* **1982**, *155*, 517–531.
(42) Taylor, A. J. *Carbohydr. Polym.* **1982**, *2*, 9–17.
(43) Walkinshaw, M. D.; Arnott, S. *J. Mol. Biol.* **1981**, *153*, 1075–1085.
(44) Erman, B.; Monnerie, L. *Macromolecules* **1986**, *19*, 2745–2750.
(45) Petrovic, Z. S.; MacKnight, W. J.; Koningsveld, R.; Dusek, K. *Macromolecules* **1987**, *20*, 1088–1096.
(46) Erman, B.; Jarry, J. P.; Monnerie, L. *Polymer* **1987**, *28*, 727–732.
(47) Bahar, I.; Yildirim Erbil, H.; Baysal, B. M.; Erman, B. *Macromolecules* **1987**, *20*, 1353–1356.
(48) Smidsrod, O.; Haug, A. *Biopolymers* **1971**, *10*, 1213–1227.